

About the Keggin Isomers: Crystal Structure of $[\text{N}(\text{C}_4\text{H}_9)_4]_4\text{-}\gamma\text{-}[\text{SiW}_{12}\text{O}_{40}]$, the γ -Isomer of the Keggin Ion. Synthesis and ^{183}W NMR Characterization of the Mixed $\gamma\text{-}[\text{SiMo}_2\text{W}_{10}\text{O}_{40}]^{n-}$ ($n = 4$ or 6)

André Tézé,* Emmanuel Cadot, Virginie Béreau, and Gilbert Hervé

Institut de Réactivité, Électrochimie et Microporosités, UMR CNRS 8637, Université de Versailles, 45 Avenue des États-Unis, 78035 Versailles Cedex, France

Received August 1, 2000

The tetrabutylammonium γ -dodecatungstosilicate has been crystallized in a 6/1 acetonitrile/water solvent. An X-ray single-crystal analysis was carried out on $[\text{N}(\text{C}_4\text{H}_9)_4]_4\text{-}\gamma\text{-}[\text{SiW}_{12}\text{O}_{40}]$ which crystallizes in the orthorhombic system, space group $P2_12_12_1$, with $a = 19.0881(3)$ Å, $b = 21.4435(3)$ Å, $c = 26.0799(1)$ Å, $V = 10674.9(2)$ Å³, $Z = 4$, and $\rho_{\text{calcd}} = 2.392$ g/cm³. The idealized C_{2v} arrangement of the anion results from the rotation of 60° of two trigonal $\{\text{W}_3\text{O}_{13}\}$ groups in the Keggin anion. Taking as reference the geometrical characteristics of the Keggin anion, it appears that the bond lengths and bonds angles within the four $\{\text{W}_3\text{O}_{13}\}$ groups are not significantly modified while the μ -oxo junctions between the two rotated groups and those between the two unrotated groups involve more acute and opened W–O–W angles, respectively. The syntheses and ^{183}W NMR characterizations of the mixed $\gamma\text{-}[\text{SiW}_{10}\text{Mo}_2\text{O}_{40}]^{n-}$ compounds corresponding to the oxidized (Mo^{VI} ; $n = 4$) and to the two electron-reduced (Mo^{V} ; $n = 6$) anions are reported. Structural analysis by ^{183}W NMR has proved unambiguously that the C_{2v} structure of the $\gamma\text{-}[\text{SiW}_{10}\text{O}_{36}]^{8-}$ subunit is retained in both the compounds. The electronic behavior of the series $\gamma\text{-}[\text{SiW}_{10}\text{M}_2\text{E}_2\text{O}_{36}]^{6-}$ ($\text{M} = \text{Mo}$ or W ; $\text{E} = \text{O}$ or S) is examined, compared and related to ^{183}W NMR data.

Introduction

Since the report of two “silicotungstic acids” with the ratio $\text{Si}/\text{W} = 1/12$,¹ isomerism of tungstosilicates has been largely studied and relations between the different members of this family have been cleared up.² Geometrical isomers of the Keggin structure result from successive 60° rotations around the 3-fold axes of the trigonal edge sharing $\{\text{W}_3\text{O}_{13}\}$ units. Baker and Figgis have reported that five isomers are theoretically possible:³ the Keggin structure and related isomers wherein one, two, three, or all four of the trigonal units have been rotated. For the dodecatungstosilicate anion, three isomers are known. The α -isomer has the well-known Keggin structure as shown by Smith on the potassium salt,⁴ Kobayashi and Sasaki on the barium salt,⁵ and Fuchs et al. on the TMA salt.⁶ Sasaki et al. established, for the first time, the structure of the β -isomer on the potassium salt,⁷ then followed by Fuchs on the TBA salt.⁸ Fuchs et al. claimed to solve the structure of “ $\gamma\text{-}[\text{PW}_{12}\text{O}_{40}]^{3-}$ ”, but it appeared that it was a crystallographic artifact due to a positional disorder.^{9,10} In a previous work, we have deduced the structure of the γ -isomer through the route of formation which consists of stereospecific addition of a ditungstic group

$\{\text{W}_2\text{O}_4\}$ to the $\gamma\text{-}[\text{SiW}_{10}\text{O}_{36}]^{8-}$ ion.¹¹ The structural analysis by ^{183}W NMR spectroscopy confirmed the expected arrangement of the γ isomer. Therefore, in keeping with these studies, we report here for the first time on the crystal structure of the γ -isomer of the dodecatungstosilicate polyanion. The careful analysis of the structure pointed out that the main changes involve the contacts between equivalent triads, i.e., the two rotated and the two unrotated groups. In addition, we present the synthesis and the ^{183}W NMR characterization of the mixed oxidized anion $\gamma\text{-}[\text{SiMo}^{\text{VI}}_2\text{W}_{10}\text{O}_{40}]^{4-}$ and the reduced analogous $\gamma\text{-}[\text{SiMo}^{\text{V}}_2\text{W}_{10}\text{O}_{40}]^{6-}$ compound. We compare herein the electronic properties of the 2-electron-reduced species of the $\gamma\text{-}[\text{SiW}_{10}\{\text{M}_2\text{E}_2\text{O}_2\}\text{O}_{36}]^{6-}$ series ($\text{M} = \text{Mo}$ or W and $\text{E} = \text{O}$ or S) which can exhibit “heteropoly brown” or “heteropoly blue” behavior.

Experimental Section

Elemental analysis was performed by the Service Central d'Analyses du CNRS.

Infrared spectra were recorded on an IRFT Magna 550 Nicolet spectrophotometer at 0.5 cm⁻¹ resolution, using the technique of pressed KBr pellets.

NMR Measurements. ^{183}W NMR spectra were recorded at 20 °C from a saturated solution in polyanion on a Bruker AC-300 spectrometer operating at 12.5 MHz in 10-mm tubes. Chemical shifts are referenced to an external 2 M Na₂WO₄ solution in alkaline D₂O, and to the α -dodecatungstosilicic acid as secondary standard ($\delta = -103.8$ ppm). The saturated aqueous solution of Li₆[SiW₁₀Mo₂O₄₀] was obtained by cationic exchange of the corresponding cesium salt through a Dowex 50W-X2 resin (Li⁺ form). The eluate was evaporated until dry and dissolved in a mixture of H₂O–D₂O (v/v) in order to obtain a concentration of about 0.8 M. The ^{183}W NMR spectrum of $\gamma\text{-}[\text{SiW}_{10}$ -

- (1) Marignac, C. *Ann. Chim.* **1862**, 25, 362.
- (2) (a) Tézé, A.; Hervé, G. *J. Inorg. Nucl. Chem.* **1977**, 39, 999. (b) Hervé, G.; Tézé, A. *Inorg. Chem.* **1977**, 16, 2115. (c) Canny, J.; Tézé, A.; Thouvenot, R.; Hervé, G. *Inorg. Chem.* **1986**, 25, 2119.
- (3) Baker, L. C. W.; Figgis, J. S. *J. Am. Chem. Soc.* **1970**, 92, 3794.
- (4) Smith, P. Ph.D. Thesis, Georgetown University, 1971; *Diss. Abstr. Int.*, B **1972**, 32, 5136.
- (5) Kobayashi, A.; Sasaki, Y. *Bull. Chem. Soc. Jpn.* **1975**, 48, 885.
- (6) Fuchs, J.; Thiele, A.; Palm, R. *Z. Naturforsch.* **1981**, 36b, 161.
- (7) Matsumoto, K. Y.; Kobayashi, A.; Sasaki, Y. *Bull. Chem. Soc. Jpn.* **1975**, 48, 3146.
- (8) Fuchs, J.; Thiele, A.; Palm, R. *Z. Naturforsch.* **1981**, 36b, 161.
- (9) Fuchs, J.; Thiele, A.; Palm, R. *Angew. Chem., Int. Ed. Engl.* **1982**, 23, 789. Fuchs, J.; Thiele, A.; Palm, R. *Z. Naturforsch., B: Anorg. Chem. Org. Chem.* **1982**, 87B, 1418.
- (10) Evans, H. T., Jr.; Pope, M. T. *Inorg. Chem.* **1984**, 23, 501.

- (11) Tézé, A.; Canny, J.; Gurban, L.; Thouvenot, R.; Hervé, G. *Inorg. Chem.* **1996**, 35, 1001.

$\text{Mo}_2\text{O}_4^{4-}$ was directly obtained from the tetrabutylammonium salt dissolved in a nonaqueous mixture of dimethylformamide- d_3 acetonitrile (2/1 v/v).

Synthesis. All chemicals were used without further purification. The tetrabutylammonium dimolybdate(VI) $[\text{NBu}_4]_2[\text{Mo}_2\text{O}_7]$, used for the synthesis of the γ - $[\text{SiW}_{10}\text{Mo}_2\text{O}_{40}]^{4-}$ anion, was prepared through the procedure reported in *Inorganic Syntheses* series.¹²

$[\text{N}(\text{C}_4\text{H}_9)_4]_4\gamma\text{-}[\text{SiW}_{12}\text{O}_{40}]$ was prepared according to a previously described method in *Inorganic Syntheses* series.¹³ The powder was recrystallized in a mixture of acetonitrile/water (6/1 v/v) at room temperature. Anal. Calcd for $\text{C}_{64}\text{H}_{144}\text{N}_4\text{SiW}_{12}\text{O}_{40}$: C, 20.00; N, 1.46; Si, 0.73; W, 57.41. Found: C, 19.56; N, 1.36; Si, 0.81; W, 55.32. IR cm^{-1} , polyoxoanion region: 1005 (w), 971 (s), 910 (vs), 872 (m), 840 (sh), 793 (vs), 768 (vs), 702, 554 (w), 538 (w), 520 (vw), 488 (vw), 462 (vw), 415 (w), 393 (m), 356 (vw), 332 (w), 303 (w), 278 (m). The X-ray powder spectrum fully agreed with the simulated one from single-crystal crystallographic data.

$[\text{N}(\text{C}_4\text{H}_9)_4]_4\gamma\text{-}[\text{SiW}_{10}\text{Mo}_2\text{O}_{40}]$. Tetrabutylammonium molybdate $[\text{NBu}_4]_2\text{Mo}_2\text{O}_7$ (0.50 g; 0.63 mmol) and $(\text{NBu}_4)_4\text{H}_4\gamma\text{-}[\text{SiW}_{10}\text{O}_{36}]$ (2 g; 0.6 mmol) were dissolved in 5 mL of acetonitrile. The resulting solution was slowly acidified by 5 mL of a 2 M HCl solution in acetonitrile. A cloudy precipitate was filtered off, and then 200 mL of ethanol was poured into the ice-cooled filtrate. The pale yellow $[\text{N}(\text{C}_4\text{H}_9)_4]_4\gamma\text{-}[\text{SiW}_{10}\text{Mo}_2\text{O}_{40}]$ compound precipitated and was dried by Et_2O (yield, based on tungsten: 60%). IR cm^{-1} , polyoxoanion region: 1006 (w), 968 (s), 916 (vs), 875 (m), 791 (vs), 556 (w), 537 (w), 415 (w), 388 (m), 334 (w), 305 (w), 282 (m). Anal. Calcd for $\text{C}_{64}\text{H}_{144}\text{N}_4\text{SiW}_{10}\text{Mo}_2\text{O}_{40}$: C, 20.94; H, 3.92; N, 1.53; Si, 0.79; W, 50.13; Mo, 5.23. Found: C, 19.90; H, 3.85; N, 1.41; Si, 1.02; W, 50.82; Mo, 4.95.

$\text{Cs}_6\gamma\text{-}[\text{SiW}_{10}\text{Mo}_2\text{O}_{40}]\cdot 8\text{H}_2\text{O}$. The preparation of the $\gamma\text{-}[\text{SiW}_{10}\text{Mo}_2\text{O}_{40}]^{6-}$ anion required a solution of Mo^{V} as the $[\text{Mo}_2\text{O}_4]^{2+}$ dimer which preparation was inspired by that reported by Sykes and co-workers.¹⁴ The synthesis of the divacant anion $\gamma\text{-}[\text{SiW}_{10}\text{O}_{36}]^{8-}$ used here as the precursor was previously described by Hervé et al.^{2c}

Preparation of the $[\text{Mo}_2\text{O}_4]^{2+}$ Dimer. The $[\text{Mo}_2\text{O}_4]^{2+}$ dimer was prepared from an aqueous solution of sodium molybdate (8.3×10^{-2} M) and H_2SO_4 (1 M) by electrochemical reduction at a platinum electrode. The degree of reduction was determined by coulometry and checked by UV-vis spectroscopy.¹⁵ The concentration in the $[\text{Mo}_2\text{O}_4]^{2+}$ dimer was determined precisely by potentiometric titration using a solution of cerium sulfate.

Formation of $\gamma\text{-}[\text{SiW}_{10}\text{Mo}_2\text{O}_{40}]^{6-}$. $\text{K}_8\gamma\text{-}[\text{SiW}_{10}\text{O}_{36}]\cdot 12\text{H}_2\text{O}$ (6 g; 2.0 mmol) was added into 50 mL of a 4.8×10^{-2} mol·L⁻¹ solution of the $[\text{Mo}_2\text{O}_4]^{2+}$ dimer. The color of the solution turned from brown-yellow to dark red-brown. Then, cesium chloride (3.5 g; 20 mmol) was added to the solution. The cesium salt $\text{Cs}_6\gamma\text{-}[\text{SiW}_{10}\text{Mo}_2\text{O}_{40}]\cdot 8\text{H}_2\text{O}$ precipitated and was isolated by filtration (yield: 90%, based on W atom). IR, cm^{-1} : 957 (s), 897 (s), 790 (vs), 728 (m), 687 (m), 624 (w), 555 (m), 491 (vw), 459 (vw), 377 (w), 356 (m), 339 (w), 330 (w), 305 (m), 279 (m). Anal. Calcd for $\text{C}_8\text{H}_{16}\text{SiW}_{10}\text{Mo}_2\text{O}_{48}$: Cs, 21.91; Si, 0.77; W, 50.49; Mo, 5.27. Found: Cs, 21.18; Si, 0.82; W, 51.12; Mo, 4.96.

X-ray Crystallography. A well-shaped colorless crystal ($0.60 \times 0.36 \times 0.30$ mm³) of $[\text{N}(\text{C}_4\text{H}_9)_4]_4\gamma\text{-}[\text{SiW}_{12}\text{O}_{40}]$ was mounted in a Lindemann tube for indexing and intensity data collection at room temperature on a Siemens SMART-CCD area detector system equipped with a normal-focus molybdenum-target X-ray tube ($\lambda = 0.71073$ Å). Intensity data were collected in 1271 frames with increasing ω (width of 0.3° per frame). Unit cell dimensions were refined by a least-squares fit on reflections. Of the 72214 reflections, 26931 unique reflections ($R_{\text{int}} = 0.1039$) and 13043 were considered [$I > 3\sigma(I)$]. Corrections for polarization and Lorentz effects were applied. An absorption

Table 1. Crystal Data and Structure Refinement for $[\text{N}(\text{C}_4\text{H}_9)_4]_4\gamma\text{-}[\text{SiW}_{12}\text{O}_{40}]$

$\text{C}_{64}\text{H}_{144}\text{N}_4\text{O}_{40}\text{SiW}_{12}$	space group $P2_12_12_1$ (No. 19)
$a = 19.0881(3)$ Å	$T = 23^\circ\text{C}$
$b = 21.4435(3)$ Å	$\lambda = 0.71073$ Å
$c = 26.07990(10)$ Å	$\rho_{\text{calcd}} = 2.392$ g·cm ⁻³
$V = 10674.9(2)$ Å ³	$\mu = 12.954$ mm ⁻¹
$Z = 4$	$^aR(F_o) = 0.0591$
$\text{fw } 3844.12$ g·mol ⁻¹	$^bR_w(F_o^2) = 0.1162$

$$^a R = \frac{\sum |F_o| - |F_c|}{\sum |F_c|}, \quad ^b R_w = \left\{ \frac{\sum [w(F_o^2 - F_c^2)]}{\sum w(F_o^2)^{1/2}} \right\}^{1/2},$$

$$1/w = \sigma^2 F_o^2 + (aP)^2 + bP.$$

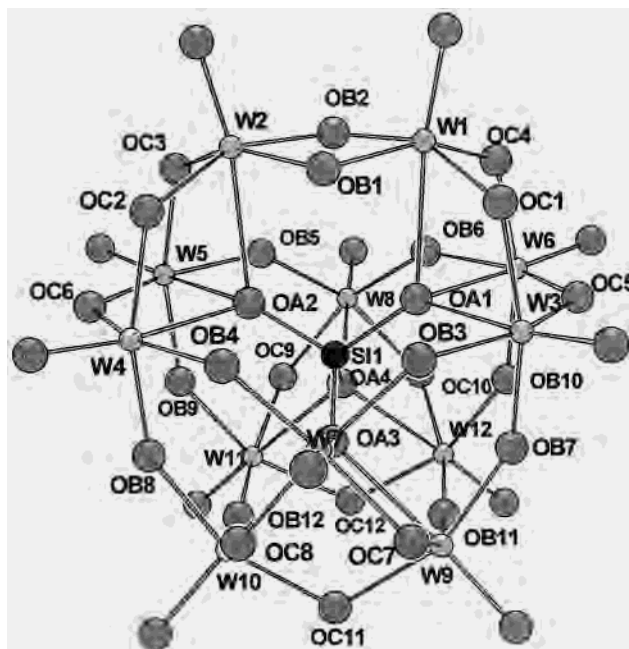


Figure 1. Atom-labeling scheme for $\gamma\text{-}[\text{SiW}_{12}\text{O}_{40}]^{4-}$ anion.

correction was performed using the SADABS program¹⁶ based on the methods of Blessing.¹⁷ The space group, $P2_12_12_1$, was determined on the basis of systematic absences and statistics of intensity distribution. Direct methods were used to locate the heaviest atoms, and then oxygen, nitrogen, and carbon atoms were found from successive refinements by full-matrix least-squares using the SHELX-TL package.¹⁸ The final refinement cycle including the atomic coordinates, anisotropic thermal parameters (atoms of the Keggin anion), and isotropic thermal parameters (atoms of the tetrabutylammonium cations) converged toward $R1 = 0.0591$, $wR2 = 0.1162$. All non-hydrogen atoms have been located except two terminal carbon atoms of tetrabutylammonium cations. Crystallographic data are given in Table 1. The anion with labeled atoms is shown in Figure 1. The tungsten atoms are numbered according to IUPAC rules.¹⁹ Different types of oxygen atoms are distinguished in the polyanion: Oa oxygen atoms are linked to the central silicon atom, and Ob and Oc oxygen atoms link $\{\text{WO}_6\}$ octahedra of two different $\{\text{W}_3\text{O}_{13}\}$ groups and within a $\{\text{W}_3\text{O}_{13}\}$ group, respectively. Od oxygen atoms are terminal ones. Selected bond lengths and angles are given in Tables 2 and 3, respectively.

Results and Discussion

Description of the Structure. The structure of the polyanion $\gamma\text{-}[\text{SiW}_{12}\text{O}_{40}]^{4-}$ is shown in polyhedral representation in Figure

(12) Hur, N. H.; Klemperer, W. G.; Wang, R.-C. *Inorg. Synth.* **1990**, *27*, 79.
 (13) Téze, A.; Hervé, G. *Inorg. Synth.* **1990**, *27*, 85.
 (14) Cayley, R. G.; Sykes, A. G. *Inorg. Chem.* **1976**, *15*, 2882.
 (15) (a) Cayley, R. G.; Taylor, R. S.; Wharton, R. K.; Sykes, A. G. *Inorg. Chem.* **1977**, *16*, 1377. (b) Sasaki, Y.; Sykes, A. G. *J. Chem. Soc., Dalton Trans.* **1974**, 1468.

(16) Sheldrick, G. M. *SADABS, program for scaling and correction of area detector data*; University of Göttingen: Göttingen, Germany, 1997.
 (17) Blessing, R. *Acta Crystallogr.* **1995**, *A51*, 33.
 (18) Sheldrick, G. M. *Acta Crystallogr.* **1990**, *A46*, 467. Sheldrick, G. M. *SHELX-TL version 5.03, Software Package for the Crystal Structure Determination*; Siemens Analytical X-ray Instrument Division: Madison, WI, 1994.
 (19) Jeannin, Y.; Fournier, M. *Pure Appl. Chem.* **1987**, *59*, 1529.

Table 2. Selected Bond Lengths (Å) for $[\text{N}(\text{C}_4\text{H}_9)_4]_4\text{-}\gamma\text{-}[\text{SiW}_{12}\text{O}_{40}]$

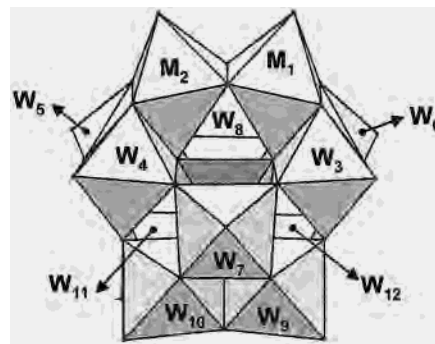
W(1)–OD1	1.723(13)	W(7)–OB3	1.933(11)
W(1)–OC1	1.895(13)	W(7)–OC7	1.946(11)
W(1)–OB2	1.906(13)	W(7)–OA3	2.359(10)
W(1)–OC4	1.907(11)	W(8)–OD8	1.707(14)
W(1)–OB1	1.947(13)	W(8)–OB6	1.885(11)
W(1)–W(2)	2.9926(12)	W(8)–OB5	1.900(13)
W(2)–OD2	1.690(13)	W(8)–OC9	1.927(11)
W(2)–OC2	1.897(12)	W(8)–OC10	1.932(12)
W(2)–OC3	1.922(13)	W(8)–OA4	2.329(11)
W(2)–OB1	1.949(13)	W(9)–OD9	1.692(13)
W(2)–OB2	1.952(14)	W(9)–OB11	1.889(13)
W(3)–OD3	1.676(13)	W(9)–OB7	1.895(11)
W(3)–OB3	1.890(12)	W(9)–OC7	1.917(11)
W(3)–OB7	1.906(11)	W(9)–OC11	1.948(13)
W(3)–OC5	1.911(14)	W(9)–OA3	2.344(11)
W(3)–OC1	1.952(11)	W(10)–OD10	1.717(12)
W(3)–OA1	2.302(11)	W(10)–OB12	1.896(12)
W(4)–OD4	1.699(14)	W(10)–OB8	1.906(12)
W(4)–OB4	1.934(12)	W(10)–OC8	1.919(12)
W(4)–OC6	1.936(14)	W(10)–OC11	1.924(13)
W(4)–OB8	1.957(11)	W(10)–OA3	2.355(10)
W(4)–OC2	1.965(13)	W(11)–OD11	1.713(13)
W(4)–OA2	2.321(12)	W(11)–OB12	1.903(12)
W(5)–OD5	1.675(13)	W(11)–OC9	1.915(13)
W(5)–OB9	1.889(13)	W(11)–OC12	1.930(12)
W(5)–OC6	1.90(2)	W(11)–OB9	1.930(14)
W(5)–OB5	1.931(13)	W(11)–OA4	2.333(11)
W(5)–OC3	1.939(13)	W(12)–OD12	1.672(13)
W(5)–OA2	2.342(12)	W(12)–OB10	1.882(11)
W(6)–OD6	1.704(13)	W(12)–OC10	1.897(11)
W(6)–OC5	1.914(13)	W(12)–OB11	1.909(13)
W(6)–OB10	1.926(12)	W(12)–OC12	1.918(11)
W(6)–OB6	1.942(12)	W(12)–OA4	2.359(11)
W(6)–OC4	1.946(11)	Si(1)–OA2	1.613(13)
W(6)–OA1	2.359(11)	Si(1)–OA1	1.620(12)
W(7)–OD7	1.67(2)	Si(1)–OA3	1.622(11)
W(7)–OB4	1.887(12)	Si(1)–OA4	1.650(12)
W(7)–OC8	1.928(11)		

Table 3. Selected Angles (deg) for $[\text{N}(\text{C}_4\text{H}_9)_4]_4\text{-}\gamma\text{-}[\text{SiW}_{12}\text{O}_{40}]$

OA2–Si(1)–OA1	111.3(6)	W(12)–OB10–W(6)	146.4(8)
OA2–Si(1)–OA3	109.5(6)	W(9)–OB11–W(12)	160.8(7)
OA1–Si(1)–OA3	109.3(6)	W(10)–OB12–W(11)	162.1(7)
OA2–Si(1)–OA4	109.2(6)	W(1)–OC1–W(3)	123.2(6)
OA1–Si(1)–OA4	110.3(6)	W(2)–OC2–W(4)	122.6(7)
OA3–Si(1)–OA4	107.2(6)	W(2)–OC3–W(5)	122.9(7)
W(1)–OB1–W(2)	100.4(6)	W(1)–OC4–W(6)	122.3(6)
W(1)–OB2–W(2)	101.7(6)	W(3)–OC5–W(6)	122.1(6)
W(3)–OB3–W(7)	145.2(6)	W(5)–OC6–W(4)	120.8(6)
W(7)–OB4–W(4)	145.9(6)	W(9)–OC7–W(7)	118.9(5)
W(8)–OB5–W(5)	144.0(7)	W(10)–OC8–W(7)	119.2(5)
W(3)–OB3–W(7)	145.2(6)	W(11)–OC9–W(8)	119.3(6)
W(9)–OB7–W(3)	147.1(7)	W(12)–OC10–W(8)	120.3(6)
W(10)–OB8–W(4)	143.2(6)	W(10)–OC11–W(9)	119.7(6)
W(5)–OB9–W(11)	146.6(7)	W(12)–OC12–W(11)	120.7(5)

2. According to its way of formation by selective addition of tungstate to the $\gamma\text{-}[\text{SiW}_{10}\text{O}_{36}]^{8-}$ precursor, it derives from the α -isomer by 60° rotations of two $\{\text{W}_3\text{O}_{13}\}$ triads around 3-fold axes. However, likely due to crystal-packing effects, the symmetry of the polyanion in the crystal (C_1) is lower than the symmetry in solution (C_{2v}) deduced from the ^{183}W NMR spectrum.¹¹

The interest of the structural determination of the “pure” γ -Keggin isomer which contains only W(VI) as metal center highlights the geometrical modifications of bond lengths and/or bond angles induced in the anion by the 60° rotations of the oxotritungstic groups. Observations of the W–Oc bond lengths [1.907(11)–1.965(13) Å] and of the W–Oc–W angles [118.9(5)–123.2(6) $^\circ$] within the triads reveal that the usual geometrical

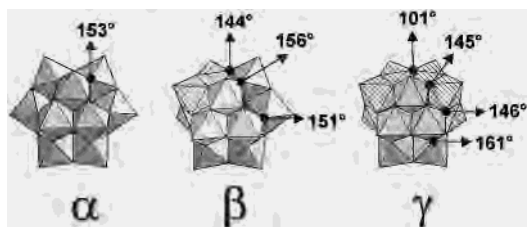
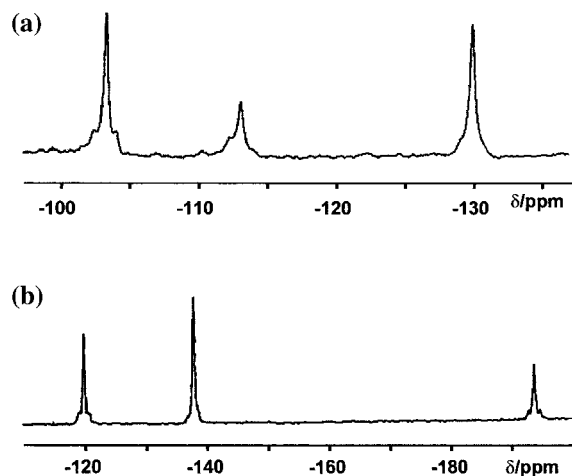
**Figure 2.** Polyhedral representation of γ -Keggin anion with the numbered tungsten atoms according to the IUPAC recommendations.

parameters pointed out for the α^{4-6} and $\beta^{7,8,20}$ anions are retained. Such groups can be considered as quasi-rigid building blocks upon the structural isomerism of the Keggin anion. On the contrary, the μ -oxo junctions between the groups involving the bridging Ob atoms appear more strongly perturbed. The W–Ob bond lengths are always in the usual range [1.900(13)–1.957(11) Å], but W–Ob–W bond angles exhibit more significant changes (see Table 3). For the α -isomer, the mean value is 153° . For the β -isomer, we use the geometrical parameters of the $\text{K}_4\text{-}\beta\text{-}[\text{SiMoW}_{11}\text{O}_{40}]\cdot 9\text{H}_2\text{O}$ structure, determined by Robert et al.,²⁰ for which the crystallographic data, the refinement parameters, and the esd's of the fractional atomic coordinates were revealed to be of better quality than those obtained by Fuchs⁸ et al. and Sasaki et al.⁷ For such a structure, the corner-shared W–Ob–W linkages corresponding to the junctions between the rotated group and the three others present more acute W–Ob–W angles ($\sim 144^\circ$) while an opening of the angles is observed for the W–Ob–W junctions involving the tungsten atoms adjacent to the rotated group (156°). No significant change is observed for the remaining corner-shared junctions located at the opposite side of the rotated group (151°). For the γ -isomer, a “true” di- μ -oxo junction involving W1 and W2 now links the two rotated groups. As expected, both the W1–Ob–W2 angles are strongly reduced [100.4(6)–101.7(6) $^\circ$] while all the W–Ob bonds, even those of the ditungstic fragment $\{\text{W}_2\text{O}_4\}$, retain the usual lengths. The eight W–Ob–W linkages between the two rotated and the two unrotated triads display more acute angles [143.2(6)–147.1(7) $^\circ$] while the two remaining corner-shared junctions W10–Ob12–W11 and W9–Ob11–W12, involving unrotated triads, exhibit pronounced angle openings [162.1(7) $^\circ$ and 160.8(8) $^\circ$]. As a consequence of the 60° rotations, the separation of the W1 and W2 atoms (2.99 Å) corresponds to the shortest distance between W(VI) atoms in a polyoxoanionic framework. The distances between tungsten atoms ensuring the linkage between rotated and unrotated groups decrease (3.643–3.658 Å) compared to the common value observed for the α -isomer (3.72 Å). The W–W separation between unrotated groups appears slightly lengthened (3.746–3.753 Å) as a consequence of the angle opening between these atoms. These observations can be understood if the four oxygen atoms labeled Oa are considered as the “kneecaps” of the all four triads. Such a situation holds because the central SiO_4 tetrahedron exhibits no significant deviation from the original T_d symmetry and can be regarded as a rigid subunit (see Table 3). Thus, bringing together the W1 and W2 atoms leads to a rocking of the two rotated groups around the Oa1 and Oa2 atoms with the consequence to open the half-structure. The two

(20) Robert, F.; Tézé, A.; Hervé, G.; Jeannin, Y. *Acta Crystallogr.* **1980**, B36, 11.

Table 4. ^{183}W NMR Data of $\gamma\text{-}[\text{SiW}_{10}\text{M}_2\text{E}_2\text{O}_{38}]^{n-}$

compound	^{183}W NMR chemical shift/ppm				ref
	M1(M2)	W7(W8)	W3(W4,W5,W6)	W9(W10,W11,W12)	
$[\text{SiW}_{10}\text{Mo}_2\text{O}_{40}]^{4-}$		-113.0	-103.2	-130.0	this work
$[\text{SiW}_{10}\text{Mo}_2\text{O}_{40}]^{6-}$		-194.5	-120.9	-138.8	this work
$[\text{SiW}_{10}\text{Mo}_2\text{S}_2\text{O}_{40}]^{6-}$		-177.0	-122.9	-145.5	25
$[\text{SiW}_{12}\text{O}_{40}]^{4-}$	-160.1	-116.8	-104.7	-127.4	11
$[\text{SiW}_{12}\text{S}_2\text{O}_{40}]^{6-}$	+1041	-184.4		-121.3 -144.6	25
$[\text{SiW}_{12}\text{O}_{40}]^{6-}$	-131.0 -124.0		-63.0	+489.0	11

**Figure 3.** Variation of the W–Ob–W angles upon the successive 60° rotations of the $\{\text{W}_3\text{O}_{13}\}$ triads.**Figure 4.** ^{183}W NMR spectra of (a) $\gamma\text{-}[\text{SiMo}_2\text{W}_{12}\text{O}_{40}]^{4-}$ and (b) $\gamma\text{-}[\text{SiMo}_2\text{W}_{10}\text{O}_{40}]^{6-}$.

unrotated groups rock around their corresponding Oa atoms for minimizing the distortions due to the original displacements of the rotated triads. Such concerted rearrangement leads to the increase of the W9–Ob11–W12 and W10–Ob12–W11 angles ensuring the linkage between the two unrotated $\{\text{W}_3\text{O}_{13}\}$ groups and to a decrease of the angles of the remaining corner-shared junctions. The variations of the angles of the corner-shared junctions in the α -, β -, and γ -isomers are highlighted in Figure 3.

^{183}W NMR Characterization. The ^{183}W NMR spectra of the disubstituted $\gamma\text{-}[\text{SiW}_{10}\text{M}_2\text{O}_{40}]^{n-}$ anions are shown Figure 4 and the corresponding NMR data summarized in Table 4. The spectrum of the oxidized mixed $[\text{NBu}_4]_4\text{-}\gamma\text{-}[\text{SiW}_{10}\text{Mo}^{\text{VI}}_2\text{O}_{40}]^{4-}$ in CD_3CN solution presents three resonance lines at -130.0 , -113.0 , and -103.2 ppm with 2:1:2 relative intensities as expected for 10 tungsten atoms involved in a C_{2v} $\gamma\text{-SiW}_{10}$ subunit. The -113.0 ppm line is assigned to the pair W7(W8). The -103.2 ppm line exhibits two degeneracy corner coupling (~ 20 Hz), identified by the relative intensity of the satellites (about 14% of the signal) and then corresponds to the four equivalent tungsten atoms W3, W4, W5, W6. The remaining resonance (-130.0 ppm) is attributed to the W9, W10, W11, W12 tungsten atoms and exhibits only one corner coupling. The features of the ^{183}W NMR spectrum of the

2-electron-reduced anion $\gamma\text{-}[\text{SiW}_{10}\text{Mo}^{\text{V}}_2\text{O}_{40}]^{6-}$ are those expected for a C_{2v} γ -isomer. The three resonance lines at -120.9 , -138.8 , and -194.5 ppm with relative intensities of 2:2:1 correspond to the 10 tungsten atoms. The chemical shifts are in the expected range for tungsten(VI) atoms in an octahedral oxo environment. On the basis of its intensity, the -194.5 ppm line is attributed to the equivalent pair W7(W8). This line is connected to the -120.9 ppm resonance through a corner coupling ($^2J_{\text{W-W}} = 23$ Hz) corresponding to the junction between W7(W8) and W3(W4, W5, W6). The -120.9 ppm, which clearly exhibits the $^2J_{\text{W-W}} = 23$ Hz, is then assigned to the four equivalent tungsten atoms W3(W4, W5, W6). The remaining line at -138.8 ppm is attributed to the W9(W10, W11, W12) tungsten atoms. This line exhibits a single corner coupling (16 Hz) corresponding to the corner-shared junctions involving the W3(W4, W5, W6) atoms.

Electronic Behavior. The ^{183}W NMR is a powerful tool to characterize the heteropoly blue or brown compounds since the W atoms that receive the localized or the thermally hopping electrons may be readily distinguished by a significant and sometimes pronounced deshielding. Pope et al. succeeded to characterize the three W^{IV} atoms ($+1500$ ppm) in the six-electron-reduced $\alpha\text{-}[\text{SiW}_9\text{W}^{\text{IV}}_3(\text{H}_2\text{O})_3\text{O}_{37}]^{4-}$ anion.²¹ Baker et al. showed that the chemical shift of the W atoms in heteropoly blue compounds may vary between about $+500$ and -300 ppm according to the residency times of the blue electrons. Such a behavior, i.e., “blue or brown”, is readily evidenced by UV–vis–near-IR spectroscopy. Intervalence charge transfer (IVCT) originates absorption in the near-IR region at ca. $1000\text{--}1300$ nm for the “blue” compounds while no absorption is observed for “brown” ones. The ^{183}W NMR study of the two-electron-reduced γ -12-tungstosilicate has revealed an asymmetric distribution for the d-electrons.¹¹ The ^{183}W chemical shifts allowed us to calculate the residency times of the two delocalized electrons over the metal centers, and we concluded that they are mainly distributed between four equivalent tungsten atoms ($\delta = +489.0$ ppm). Such asymmetric distribution of the electrons in reduced polyoxotungstates has been previously reported for the 2e-reduced species $\alpha\text{-}[\text{P}_2\text{W}_{18}\text{O}_{62}]^{6-}$ ²² and $[\text{W}_{10}\text{O}_{32}]^{6-}$ ²³ and has been explained by Borshch in terms of correlated thermal delocalization of the two electrons over the W atoms forming two central belts.²⁴ Each electron hops on the W atoms of one belt, both the exchanges being coupled via quasi-linear μ -oxo bridges which ensure the connection between the two equivalent belts. Similar conditions may also be encountered for the γ -isomer, and such an explanation could be proposed for the two delocalized electrons in the $\gamma\text{-}[\text{SiW}_{12}\text{O}_{40}]^{6-}$ species. Among the two groups of four equivalent W

(21) Pieprgrass, K.; Pope, M. T. *J. Am. Chem. Soc.* **1987**, *109*, 1587.(22) Kosik, M.; Hammer, C. F.; Baker, L. C. W. *J. Am. Chem. Soc.* **1986**, *108*, 2748.(23) Duncan, D. C.; Hill, C. L. *Inorg. Chem.* **1996**, *35*, 5828.(24) Borshch, S. A. *Inorg. Chem.* **1998**, *37*, 3116.

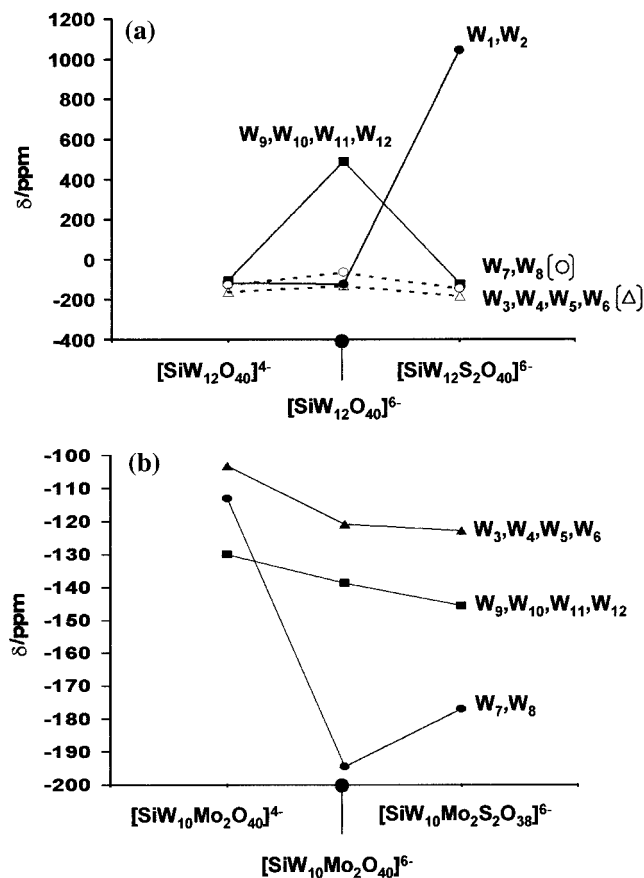


Figure 5. Plot of the ^{183}W chemical shifts of (a) $\gamma\text{-}[\text{SiW}_{12}\text{E}_2\text{O}_{38}]^{n-}$ and (b) $\gamma\text{-}[\text{SiMo}_2\text{W}_{10}\text{E}_2\text{O}_{38}]^{n-}$.

atoms, the W9–W10–W11–W12 atoms are adjacent and form two equivalent pairs connected via the largest W–Ob–W angles

[160.8(7)–162.1(7)°]. Each electron should be mainly and equally distributed over each pair (W9–W12 and W10–W11) and together hops as in a “well-adjusted” ballet. In addition, the $\text{W}^{\text{V}} \rightarrow \text{W}^{\text{VI}}$ IVCT gives rise to absorption at ca. 1280 nm. When the two Ob1 and Ob2 atoms are formally replaced by two sulfur atoms to give the isoelectronic anion $\gamma\text{-}[\text{SiW}_{12}\text{S}_2\text{O}_{38}]^{6-}$, the color of the anion changes from blue to brown as observed in the UV–vis–near-IR spectrum by the disappearance of the IVCT absorption.²⁵ This observation is supported by the ^{183}W NMR data since the deshielded peak at +1041 ppm corresponds to the pair of tungsten(V) atoms forming the $\{\text{W}_2\text{O}_2\text{S}_2\}$ fragment; the other resonance lines are in the expected range for W(VI) in an octahedral oxo environment. These results are in agreement with two d-electrons strongly localized in the vicinity of W1 and W2 atoms. The X-ray structural analysis has revealed a short distance between W1 and W2 [2.815(1) Å], characteristic of a metal–metal bond involving both the W(V) centers. Variations of the ^{183}W chemical shifts in the series $\gamma\text{-}[\text{SiW}_{12}\text{E}_2\text{O}_{38}]^{n-}$ are represented in Figure 5a. For the disubstituted compounds $\gamma\text{-}[\text{SiW}_{10}\text{Mo}_2\text{E}_2\text{O}_{38}]^{6-}$, the ^{183}W NMR and the UV–vis–near-IR results are consistent with the two added electrons trapped on the two Mo centers, involved in a metal–metal interaction.²⁵ The ^{183}W chemical shifts of the mixed reduced anions appear only slightly shielded as commonly observed when the charge of the anion increases (Figure 5b).

Supporting Information Available: An X-ray crystallographic file in CIF format for the structure of $[\text{N}(\text{C}_4\text{H}_9)_4]_4\text{-}\gamma\text{-}[\text{SiW}_{12}\text{O}_{40}]$. This material is available free of charge via the Internet at <http://pubs.acs.org>.

IC000864L

(25) Cadot, E.; Béreau, V.; Halut, S.; Sécheresse, F. *Inorg. Chem.* **1996**, *35*, 551.